Journal of Applied Polymer Science

Morphology and molecular mobility of plasticized polylactic acid studied using solid-state ^{13}C- and ^{1}H-NMR spectroscopy

Mária Kovaľaková,[1] Dušan Olčák,[1] Viktor Hronský,[1] Peter Vrábel,[1] Oľga Fričová,[1] Ivan Chodák,[2] Pavel Alexy,[3] Gabriel Sučik[4]

[1]Department of Physics, Faculty of Electrical Engineering and Informatics, Technical University of Košice, Park Komenského 2, 042 00, Košice, Slovakia

[2]Polymer Institute, Slovak Academy of Sciences, Dúbravská cesta 9, 845 41, Bratislava, Slovakia

[3]Institute of Natural and Synthetic Polymers, Slovak University of Technology, Radlinského 9, 812 37, Bratislava, Slovakia

[4]Department of Ceramics, Faculty of Metallurgy, Technical University of Košice, Park Komenského 19, 042 00, Košice, Slovakia

Correspondence to: M. Kovaľaková (E-mail: Maria.Kovalakova@tuke.sk)

ABSTRACT: MAS ^{13}C-NMR measurements were used for the study of morphology and molecular mobility in amorphous quenched and triacetine-plasticized PLA samples and PLA samples which underwent cold crystallization during annealing at 80 and 100 °C. The single pulse MAS ^{13}C-NMR spectra indicate that plasticizer promotes cold crystallization which results in the decrease of the temperature of crystallization and formation of more perfect crystalline domains. The $T_1(^{13}C)$ spin-lattice relaxation times show that the presence of plasticizer molecules leads to an increase of local mobility in PLA chains but plasticized PLA after annealing at 100 °C shows more rigid structure. The series of broad line ^{1}H-NMR spectra performed at temperatures up to 100 °C provided information on the changes in relaxation processes and morphology of the studied samples. The interpretation of the results obtained using the techniques of NMR spectroscopy were supported by WAXD and DSC measurements. © 2016 Wiley Periodicals, Inc. J. Appl. Polym. Sci. **2016**, *133*, 43517.

KEYWORDS: biodegradable; crystallization; morphology; plasticizer; spectroscopy

Received 20 August 2015; accepted 4 February 2016

DOI: 10.1002/app.43517

INTRODUCTION

Biodegradable polymers exhibit a wide range of remarkable properties and can compete with non-biodegradable thermoplastics in various fields.[1,2] Aliphatic polyesters, among which polylactic acid (PLA)[3,4] also belongs, are well-known biocompatible and biodegradable polymers which are considered to be an alternative to nondegradable bio-resistant polymers. PLA exhibits a remarkable balance of performance properties, which are comparable to traditional thermoplastics. The physical properties of PLA, which strongly depend on its crystalline structure and morphology, can be effectively altered through the crystallization process. Depending on the crystallization conditions, PLA forms various polymorphic crystalline structures[5–12]; the most common and most stable α-modification with the 10_3 helix is usually formed under melt, cold and solution crystallization. Both the degree of crystallinity and microscopic morphology of PLA strongly depend on the thermal history and can be manipulated applying a thermal treatment of the virgin polymer material, consisting in either annealing, or melting and annealing or by melting, quenching and annealing of PLA at different temperatures.[13–15] However, some of the PLA properties limit its applicability, mainly when considering low thermal stability at processing temperatures, brittleness and relatively low impact strength.[16] One of the ways to improve PLA properties is the incorporation of additives (such as plasticizers) into the polymer.[17,18] Triacetine (glycerol triacetate, TAC) is a common low molecular weight compound which has proved to be an effective plasticizer when blended with PLA. The effects of TAC on the dynamic mechanical and thermal properties of PLA[19,20] and on crystallization, chain mobility, microstructure, and tensile properties of PLA[21] have been studied. Wide angle X-ray diffraction (WAXD) measurements showed that PLA plasticized with the TAC amount up to the weight of 30% retains its amorphous structure when cooled down from 190 °C to ambient temperature. On the other hand, annealing of amorphous plasticized sample at the heating rate of 3 °C/min up to 90 °C resulted in the XRD pattern with peaks characteristic for α form PLA crystals whose magnitude increases with increasing amount of plasticizers.[21] The cosolvent blending of PLA with increasing amounts of plasticizers resulted in materials with increasing crystallinity. Their WAXD patterns display peaks characteristic for α form PLA.[20] These results confirmed that

crystallization process in PLA is facilitated by the presence of compatible plasticizers which, in general, increase the free volume and molecular mobility of the plasticized samples. These effects were also detected in DSC experiments. Typical DSC thermograms of PLA[15,20,22–24] display the glass transition above 55 °C, exothermal peak between 80 and 140 °C related to the cold crystallization process and the melting endotherm often as a double peak between 140 and 180 °C. The presence of TAC leads to the significant drop in the temperatures of glass transition and cold crystallization, slightly decreased melting temperature and accelerated cold crystallization process as a consequence of chain flexibility and free volume increase and decrease in intermolecular attraction as the TAC molecules penetrate into PLA chains.[18,21]

The NMR spectroscopy, which is a powerful tool for the study of the structure and molecular dynamics in polymers, was also used for the study of PLA structure. The solid-state MAS ^{13}C-NMR spectra for amorphous, crystalline and semicrystalline PLA samples are preferably detected using the cross-polarization (CP) NMR technique[22,25–29] since the sufficient signal to noise ratio in the CP MAS ^{13}C-NMR spectra can be obtained during much shorter time than the time which is needed for the single pulse (SP) MAS ^{13}C-NMR spectra. On the other hand, in general, only the latter measurements reflect the polymer structure quantitatively. The broad lines related to the CH_3, CH and CO carbons of amorphous PLA and the sharp peaks superimposed on the broad lines related to particular carbons in crystalline domains are characteristic for the spectra of semicrystalline PLA detected by both NMR techniques. The NMR crystallography revealed 10 nonequivalent CH_3, CH and CO carbons in the crystal structure of the α-polymorph of PLA.[30]

A single pulse ^{1}H-NMR applied within a broad temperature range provides information on local motions in polymer chains.[31] In general, the shape of the solid-state NMR spectra is influenced by the interactions in which the examined nuclei are involved. The solid-state ^{1}H-NMR spectra are broad especially owing to a strong direct dipolar interaction among protons and the broad-line ^{1}H-NMR spectra measured at the MAS frequency of about 2.5 kHz at room frequency for PLA show one unstructured broad line.[32] Molecular motion in the studied material averages out anisotropic interactions and to some extent the dipolar interactions as well, which gives rise to a narrowing of the solid-state NMR spectra.[33,34]

The NMR relaxation times, which provide information on molecular dynamics in the studied material, depend on the molecular composition, morphology and production process. Molecular dynamics of PLA with different morphological forms were analyzed using the ^{13}C spin-lattice relaxation times measured for CO and CH carbons at temperatures below T_g.[22,28] The spin-lattice relaxation decays measured for semicrystalline PLA were analyzed into two components related to the crystalline and amorphous regions of PLA. However, two different carbon spin-lattice relaxation times were also found for the quenched amorphous PLA identifying the existence of differently restricted states of chains with high and low chain mobility.[28]

The changes in the morphology and molecular dynamics of the virgin pelletized PLA due to annealing at the temperature within region of cold crystallization were recently studied with the use of the solid-state NMR techniques. The narrowing of the conformation distribution within amorphous and crystalline domains, an increase in the lamellae thickness and the crystallinity increase of the PLA sample were the main observed effects.[35]

As mentioned above, the characterization of PLA plasticized with TAC was carried out mainly using the DSC and WAXD techniques,[15,18–21] however, according to our best knowledge such study has not yet been performed with the solid-state NMR techniques. The main aim of this paper is therefore to characterize the morphology and molecular mobility of PLA and plasticized PLA samples prepared by annealing at temperatures which are within the region of cold crystallization of PLA using NMR spectroscopy. High-resolution ^{13}C-NMR and broad-line ^{1}H-NMR spectra, as well as carbon spin-lattice relaxation times $T_1(^{13}C)$ measured via ^{1}H-^{13}C cross-polarization (CP) NMR, provided information on the influence of plasticization with TAC on the crystallization process and morphology of PLA samples. The interpretation of the results obtained using NMR spectroscopy is supported by WAXD and DSC measurements performed on the studied samples.

EXPERIMENTAL

Materials

All samples used for the NMR measurements were prepared from the virgin pelletized PLA 4042D (PLA-V), Nature Works. The number-average molecular weight (M_n), polydispersity index (M_n/M_w), and intrinsic viscosity of PLA were 74×10^3 g/mol, 1.40 and 0.56 dl/g, respectively. Measurements were performed on the following PLA samples: PLA-Q prepared by melting PLA-V in a twin-screw extruder at 190 °C then quenching in cold water, PLA-T prepared by melting PLA-V together with TAC and then quenching under the same conditions as those for the PLA-Q sample. The PLA-T sample contained 10.0 wt. % of TAC. PLA-Q(80), PLA-Q(100), and PLA-T(80), PLA-T(100) samples were prepared by annealing of PLA-Q and PLA-T for 2 days at 80 and 100 °C, respectively.

Measurements of ^{13}C-NMR and ^{1}H-NMR Spectra

The high-resolution single-pulse (SP) MAS ^{13}C-NMR and broad-line (BL) ^{1}H-NMR measurements were performed on a Varian 400-MHz NMR spectrometer (Palo Alto, CA). The SP MAS ^{13}C-NMR spectra were recorded at the resonance frequency of approximately 100 MHz with the use of 4 mm ZrO_2 rotors and MAS frequency of 10 kHz at temperatures inside the rotor of 31 °C. Free induction decay (FID) was recorded after a radio-frequency $\pi/2$ pulse of 2.0-μs duration, with SPINAL pulse high-power proton decoupling of 90 kHz[36] and recycle delay of 120 s. The spectral width and acquisition time were 50 kHz and 20 ms, respectively. The SP MAS ^{13}C-NMR spectrum was obtained using Fourier transformation of the FID, which was an average of 1400–1500 scans.

A high-resolution ^{13}C-NMR spectrum for pure triacetine was measured at the resonance frequency of 150 MHz on a liquid-

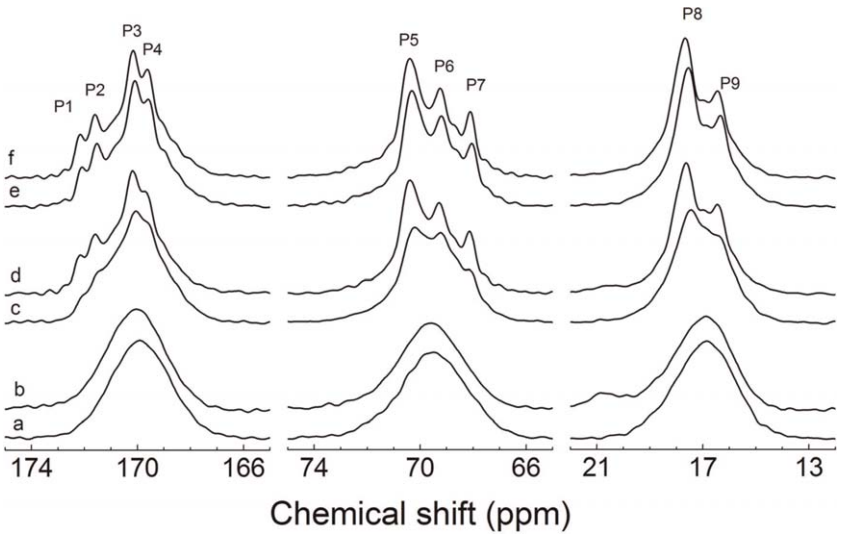

Figure 1. SP MAS ^{13}C-NMR spectra measured at 31 °C for (a) PLA-Q, (b) PLA-T, (c) PLA-Q(80), (d) PLA-T(80), (e) PLA-Q(100), and (f) PLA-T(100).

state Varian 600-MHz NMR spectrometer. TAC diluted in $CDCl_3$ was used for the measurement of the ^{13}C-NMR spectrum.

The BL ^{1}H-NMR spectra were recorded at the resonance frequency of approximately 400 MHz by means of a procedure suppressing the probehead background proposed by Chen.[31] In this procedure the free induction decay (FID) was recorded with a recycle delay of 10 s after radio-frequency pulses with durations of 1.5 and 3 μs corresponding to $\pi/4$ and $\pi/2$ pulse, respectively. The spectral width was 100 kHz and the acquisition time was modified according to the duration of the FID signal varying with the temperature from 20 to 80 ms. Each spectrum was an average of 16 scans. Spectra were measured at room temperature and elevated temperatures up to 100 °C. The sample temperature was stabilized for 20 minutes before each NMR measurement.

The chemical shifts were referenced to tetramethylsilane using adamantane as an external standard. Deconvolutions and processing of the spectra were carried out with the use of MestReNova software.

Measurements of Carbon Spin-Lattice Relaxation Times $T_1(^{13}C)$

Spin-lattice relaxation times $T_1(^{13}C)$ were measured at 31 °C using the ^{1}H-^{13}C cross-polarization (CP) MAS NMR technique according to Torchia.[37] The measurements were performed at the MAS frequency of 10 kHz, the durations of the ^{1}H and ^{13}C $\pi/2$ pulses were 2.8 and 4.8 μs, respectively, the Hartmann–Hahn condition was obtained with radio frequency field strength of 60 kHz, contact time of 2 ms, acquisition time of 20 ms, and the delay between two consecutive scans of 6 s. A pulse high-power proton decoupling field of 90 kHz was applied during the data acquisition. The T_1 (^{13}C) related to the respective peaks were found by fitting the amplitudes of the peaks detected after the recovery time, which increased up to 300 s. About 256 scans were used to measure the $T_1(^{13}C)$ array spectra.

WAXD Measurements

WAXD was carried out on an X-ray diffractometer Rigaku MiniFlex 600 using CuKα-radiation in Theta/2Theta Bragg-Brentano geometry. Accelerating voltage of 40 kV and current of 15 mA were set. The samples were scanned in range of 2Θ 5–40° by 1°/min scan speed and step 0.01°.

DSC Measurements

The DSC thermograms of PLA-Q and PLA-T samples were measured on NETZSCH STA 449 F3 instrument. Each sample was put into corundum crucible and heated up at the rate of 5 °C/min in the synthetic air atmosphere in the temperature range from 20 to 200 °C. As a reference, an empty corundum crucible was used.

RESULTS AND DISCUSSION

Single-Pulse MAS ^{13}C-NMR Spectra

The SP MAS ^{13}C-NMR spectra for quenched PLA-Q, plasticized PLA-T and annealed PLA-Q(80), PLA-Q(100), PLA-T(80) and PLA-T(100) samples are depicted in Figure 1 which demonstrates the crystallization processes in quenched and plasticized PLA samples. Both annealing temperatures are in the region of cold crystallization of PLA. The NMR spectrum of PLA-Q sample [Figure 1(a)] displays only broad singlet Gaussian lines characteristic for amorphous PLA[27,37] with widths of 247, 276, and 249 Hz assigned to carbonyl (CO) (169.9 ppm), methine (CH) (69.5 ppm), and methyl (CH_3) (16.9 ppm) carbons of PLA-Q. The spectrum of plasticized PLA-T sample [Figure 1(b)] is very similar to the one of PLA-Q sample but besides the Gaussian line related to CH_3 carbons with the maximum at 16.9 ppm, a broad shoulder on the high-frequency side at about 20.8 ppm is also seen. Based on the liquid-state ^{13}C-NMR spectrum of TAC, which displays two peaks of methyl carbons at chemical shifts of 20.87 and 20.68 ppm (Figure 2), this line can be assigned to the TAC methyl carbons. The lines related to other groups in TAC molecules cannot be found in the PLA-T spectrum due to their strong broadening and/or due to their

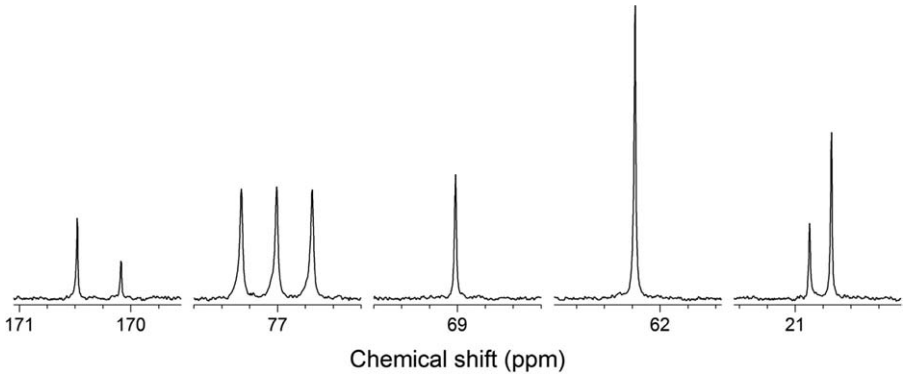

Figure 2. High-resolution liquid-state ^{13}C-NMR spectrum measured for TAC. The peaks are related to the CO (170.49 and 170.09 ppm), CH (69.02 ppm), CH_2 (62.23 ppm), and CH_3 (20.87 and 20.68 ppm) carbons. The triplet with the lines at 77.33, 77.01, and 76.69 ppm comes from carbons of the $CDCl_3$ solvent. An identical scale was used for all parts of the spectrum.

superposition with the lines related to the CH or CO carbons in PLA structure.

After annealing at 80 °C peaks and shoulders appeared in the ^{13}C-NMR spectrum of PLA-Q(80) sample. They are superimposed on the broad lines in the spectra and give evidence of the structural changes within PLA sample [Figure 1(c)]. These peaks and shoulders are in the positions of peaks of the CP MAS ^{13}C-NMR spectrum measured for the crystalline α form of PLA.[22] The spectrum of PLA-T(80) sample displays well-resolved peaks associated with crystalline domains from which can be deduced that TAC plasticizer facilitates and accelerates α-crystalline domain formation in PLA during annealing [Figure 1(d)].

The spectra of PLA-Q(100) [Figure 1(e)] and PLA-T(100) [Figure 1(f)] samples do not show conspicuous changes in the line shapes in comparison with the spectrum of PLA-T(80) sample [Figure 1(d)]. The only difference consists in diminishing of the line at 20.5 ppm related to the TAC methyl groups. This line gradually disappears with the increasing annealing temperature. The observed change in the shape of the CH_3 resonance indicates the migration of TAC molecules due to the proceeding crystallization[19] and their leakage from the sample during annealing.

To obtain information concerning morphology of annealed samples, deconvolution of the CH and CH_3 resonance lines of the SP MAS ^{13}C-NMR spectra measured for the PLA-Q(100) and PLA-T(100) was carried out into Lorentzian and Gaussian lines related to carbons within crystalline and amorphous domains respectively by the approach used in our previous research.[35] The positions of the fitted lines were taken from the positions of the narrow Lorentzian P5–P9 (Figure 1) and broad Gaussian lines in the spectra measured for annealed and quenched PLA samples respectively. The widths and intensities of the lines were obtained using the fitting procedure and are shown in Table I. The interpretation of the data is based on the above-mentioned fact that the TAC molecules partially leaked from the PLA-T(100) sample during annealing and so there is no or only negligible contribution of the TAC carbons to the resonance lines detected for this sample.

As seen in Table I, the spectrum of plasticized PLA-T(100) shows narrower lines associated with carbons within crystalline and amorphous domains in comparison with those in the spectrum of nonplasticized PLA-Q(100) sample. The narrower lines can be explained by the narrower chain conformations distribution within amorphous and crystalline domains, while narrower peaks associated with crystalline domains also indicate a formation of thicker lamellae.[25,35] Based on the results of NMR crystallography obtained for the PLA structure,[24] the CH resonance of α-crystals consists of three lines with intensities which are in the ratios 3:1:1. The intensities of the P5 – P7 peaks for PLA-T(100) sample (Table I) are in a reasonable agreement with this result indicating that the crystalline domains in PLA-T(100) sample are more perfect than in PLA-Q(100) sample. The crystallinities X_c of PLA-T(100) and PLA-Q(100) do not differ considerably.

Table I. Data Obtained from Deconvolutions of CH and CH_3 Resonances of the SP MAS ^{13}C-NMR Spectra Measured for PLA-Q(100) and PLA-T(100) Samples Measured at 31 °C—the Widths of the Peaks Associated with the Amorphous (P_{am}) and Crystalline (P5–P9) Domains, Crystallinities X_c and Relative Integral Intensities I_c of the Peaks Associated with Crystalline domains

	Methine carbons								Methyl carbons					
	Width (Hz)					I_c			Width (Hz)				I_c	
	P_{am}	P5	P6	P7	X_c	P5	P6	P7	P_{am}	P8	P9	X_c	P8	P9
PLA-Q(100)	261	76	86	52	0.67	3.6	2.3	1	250	135	92	0.68	3	1
PLA-T(100)	237	73	58	48	0.62	2.9	1.1	1	232	85	72	0.65	2.8	1

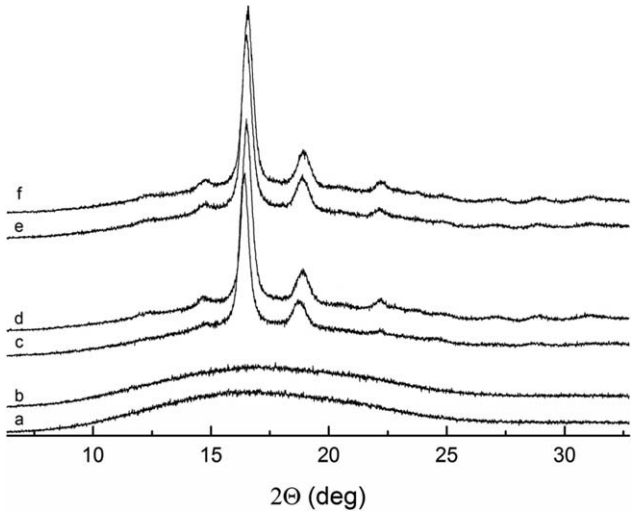

Figure 3. WAXD patterns measured at room temperature for (a) PLA-Q, (b) PLA-T, (c) PLA-Q(80), (d) PLA-T(80), (e) PLA-Q(100), and (f) PLA-T(100).

The amorphous structure of PLA-Q and PLA-T samples and the presence of crystalline domains in the annealed PLA samples were also confirmed by WAXD measurements (Figure 3).

A broad signal centered at $2\Theta = 16.5°$ observed in the WAXD patterns of both PLA-Q and PLA-T samples [Figure 3(a,b)] proved amorphous structure of these samples. The WAXD patterns of annealed samples display the peaks at 14.6°, 16.5°, 18.8°, and 22.1° which are characteristic for α form PLA crystals. The magnitudes of these peaks slightly increase with increasing annealing temperature, the most pronounced increase can be observed for the peak at 14.6°. This can be explained by the presence of more perfect α form PLA crystals, as was already deduced from MAS ^{13}C-NMR spectra.

The annealing of the PLA-T sample resulted in semicrystalline samples which due to the leakage of TAC molecules are expected to have the physical properties of not plasticized semicrystalline PLA.

Spin-Lattice Relaxation Times $T_1(^{13}C)$

Measurements of the spin-lattice relaxation times $T_1(^{13}C)$ were carried out for amorphous PLA-Q and PLA-T and semicrystalline PLA-Q(100) and PLA-T(100) samples. The $T_1(^{13}C)$ values for amorphous PLA-Q and PLA-T samples were estimated from the amplitudes of the CO, CH and CH_3 resonances observed at 169.9, 69.5 and 16.9 ppm, respectively, in the measured array. The best fit for the curve of spin-lattice relaxation of CO carbons was achieved with an exponential function and a bi-exponential function provided a reasonable fit for the CH and CH_3 curves. The curves of spin-lattice relaxation for PLA-Q sample are shown in Figure 4 and the fitted data are listed in Table II.

The relaxation rate which is inversely proportional to the relaxation time depends both on the strength of the magnetic interactions of the ^{13}C nuclei with those of ^{1}H and on fluctuations in the local magnetic fields produced by protons, whereby the former depend on the inter-nuclear distance between ^{13}C and ^{1}H and the latter are determined by molecular mobility. In agreement with previously published results,[35] the CO carbons exhibit lower relaxation rate compared to those of CH and CH_3 carbons because of weak dipolar interactions, the strength of which is determined only by the nonbonded intra- and interchain ^{1}H nuclei. The relaxation rate of CH and CH_3 carbons is predominantly determined by fluctuations in local magnetic fields produced by directly-bonded protons.

The spin-lattice relaxation time $T_1(^{13}C)$ data indicate that CO carbons in the PLA-Q relax exponentially with a single relaxation time $T_1(^{13}C)$. The $T_1(^{13}C)$ value of 53.0 s for the PLA-Q sample is very close to the $T_1(^{13}C)$ of 54.1 s estimated using the KWW function[22] as well as to the value 54.6 s of the longer relaxation time of the bi-exponential spin-relaxation decay[28] reported for amorphous PLA.

Concerning the PLA-T sample, the amount of 9.9% of TAC carbonyl carbons is present in the PLA-T material and the lines for CO carbons of PLA and TAC overlap in the ^{13}C-NMR spectrum as evident in Figures 1 and 2. In spite of that, a mono-exponential function was sufficient to fit the spin-lattice relaxation curve indicating that PLA and TAC carbonyl carbons have about the same relaxation rate.

As seen from the data in Table II, the plasticization results in a significant change in the relaxation rate of all carbons in PLA structure. Relaxation rate enhancement for CO carbons in PLA-T sample in comparison with PLA-Q sample can be explained by local mobility enhancement within polymer chains induced by the presence of mobile TAC molecules.[18]

As mentioned above, bi-exponential functions had to be fitted to the CH spin-lattice relaxation curve which means that in spite of amorphous nature of the sample, the CH carbons relax at two different rates. The complex structure containing both the standard amorphous regions and amorphous regions with parts more or less ordered in the chain aggregations elucidate bi-exponential behavior.[24] A common feature of both samples is

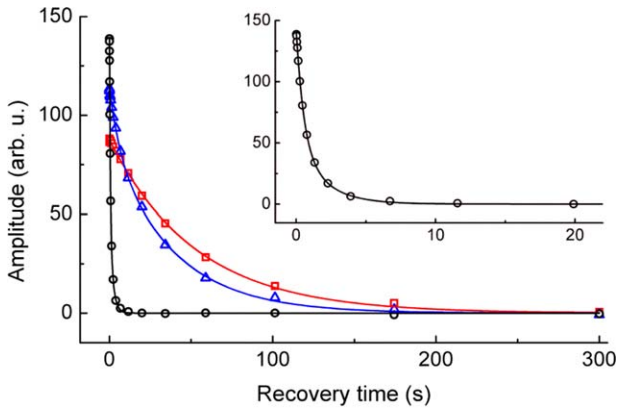

Figure 4. Decrease in amplitudes for CO (□), CH (Δ), and CH_3 (○) carbon resonances in dependence on the recovery time in the spin-lattice relaxation time $T_1(^{13}C)$ measurement for PLA-Q at 31 °C. The solid lines represent the best fits. The insert shows the initial part of CH_3 curve in a detailed view. [Color figure can be viewed in the online issue, which is available at wileyonlinelibrary.com.]

Table II. The ^{13}C Spin-Lattice Relaxation Times $T_{1,l}$ and $T_{1,s}$ and Intensities P_l and P_s Inserted in Parentheses, Estimated from the Spin-Lattice Relaxation Curves Measured for Amorphous PLA-Q and PLA-T and Crystalline PLA-Q(100) and PLA-T(100) Samples at 31 °C

		CO			CH			CH_3		
		P1	P2	P3	P5	P6	P7	P8	P9
PLA-Q	$T_{1,l}$ (s)		53.0 ± 0.7			38.3 ± 1.9 (0.77)			1.96 ± 0.18 (0.35)
	$T_{1,s}$ (s)					6.3± 1.1 (0.23)			0.54 ± 0.03 (0.65)
PLA-T	$T_{1,l}$ (s)		41.0 ± 0.7			31.5 ± 1.1 (0.72)			2.2 ± 0.4 (0.22)
	$T_{1,s}$ (s)					7.2 ± 0.7 (0.28)			0.59 ± 0.04 (0.78)
PLA-Q(100)	$T_{1,l}$ (s)	93.4 ± 1.6	80.0 ± 2.0	70.5 ± 0.9	49.3 ±2.8 (0.71)	52.4 ± 2.1 (0.72)	52.7 ± 2.9 (0.70)	1.27 ± 0.09 (0.72)	1.45 ± 0.22 (0.41)
	$T_{1,s}$ (s)				9.6 ± 1.8 (0.25)	10.8 ± 1.1 (0.30)	7.5 ± 1.5 (0.24)	0.39 ± 0.09 (0.28)	0.32 ± 0.02 (0.59)
PLA-T(100)	$T_{1,l}$ (s)	107.6 ± 3.6	92.0 ± 4.5	81.1 ± 1.5	52.1 ± 3.2 (0.71)	48.9 ± 2.7 (0.72)	52.6 ± 3.2 (0.70)	1.58 ± 0.29 (0.48)	1.24 ± 0.11 (0.46)
	$T_{1,s}$ (s)				9.4 ± 1.6 (0.29)	9.2 ± 1.5 (0.28)	10.4 ± 1.7 (0.30)	0.61 ± 0.11 (0.52)	0.31 ± 0.03 (0.54)

Relaxation times $T_{1,l}$ and $T_{1,s}$ and intensities P_l and P_s are associated with the long (l) and short (s) components of the spin-lattice relaxation curves. Only one relaxation time $T_1(^{13}C)$ was found for the CO carbons.

that spin-lattice relaxation times of CH carbons are shorter than those of CO carbons due to the presence of one directly bonded ^1H nucleus in CH groups resulting in stronger ^1H-^{13}C dipolar interactions. The long $T_{1,l}$ and short $T_{1,s}$ relaxation times obtained from the fitting procedure differ significantly, and a larger relative amount of CH carbons relates to a longer spin-lattice relaxation time. The values of a short relaxation time $T_{1,s}$ are the same for PLA-Q and PLA-T samples within the limits of errors and they can be associated with very fast relaxing CH carbons in chain sections, the motion of which is not hindered by chain aggregations. The TAC methine carbon peak, which overlaps with the PLA methine carbon peaks, is related only to 3.5% of the CH carbons in the PLA-T sample. The data in Table II show that none of the relaxation times can be attributed only to the TAC carbons but the intensity increase of the short relaxation time $T_{1,s}$ for PLA-T as compared to that of PLA-Q shows that triacetine CH carbons relax with the same rate as the fast relaxing CH carbons of PLA-Q. The effect of plasticization is visible in the long component of CH carbon spin-lattice relaxation. The smaller values of spin-lattice relaxation times $T_{1,l}$ for the PLA-T sample than for the PLA-Q sample also confirmed that plasticization results in the local chain motion enhancement and the free volume increase within plasticized PLA-T could explain this change.

The data drawn from the CH_3 spin-lattice relaxation curve are rather different from those obtained from the CO and CH carbons. The $T_1(^{13}C)$ values for the methyl carbons are one or two orders lower than those for the CO and CH carbons in all samples (Table II). The distinct increase in the relaxation rate can be attributed to rapidly fluctuating magnetic fields produced by three bonded ^1H nuclei and fast rotation of CH_3 side-chain group. As mentioned above, in the case of the PLA-T sample the CH_3 carbons of TAC form the broad shoulder on the high frequency side of the CH_3 carbon line and therefore the CH_3 spin-lattice relaxation is detected only on CH_3 carbons within PLA structure. The data for the PLA-Q and PLA-T samples show that the plasticization has no substantial influence on CH_3 carbon relaxation in both studied samples. The longer components of $T_1(^{13}C)$ for CH_3 are of lower intensity which is approximately the same as the intensity of $T_1(^{13}C)$ of shorter components of CH carbons. An occurrence of the cross-point in the temperature dependences of the long $T_{1,l}$ and short $T_{1,s}$ relaxation times with the reversed intensities related to the $T_{1,l}$ and $T_{1,s}$ observed at temperatures below and above the cross point could explain this change. Therefore, it is evident from the relaxation times estimated for PLA-Q and PLA-T samples that the plasticization has no influence on the side CH_3 group motion and TAC affects only the motion of the main chain carbons.

The $T_1(^{13}C)$ values for semi-crystalline PLA-Q(100) and PLA-T(100) samples were determined from the amplitudes of the observed peaks superposed on the broad lines in the spectra. As mentioned above, the leakage of the TAC molecules from the sample throughout the annealing was identified in the SP MAS ^{13}C-NMR spectra and for this reason PLA-Q(100) and PLA-T(100) can be considered as identical samples. The spin-lattice relaxation times $T_1(^{13}C)$ measured for carbons in CH and CH_3

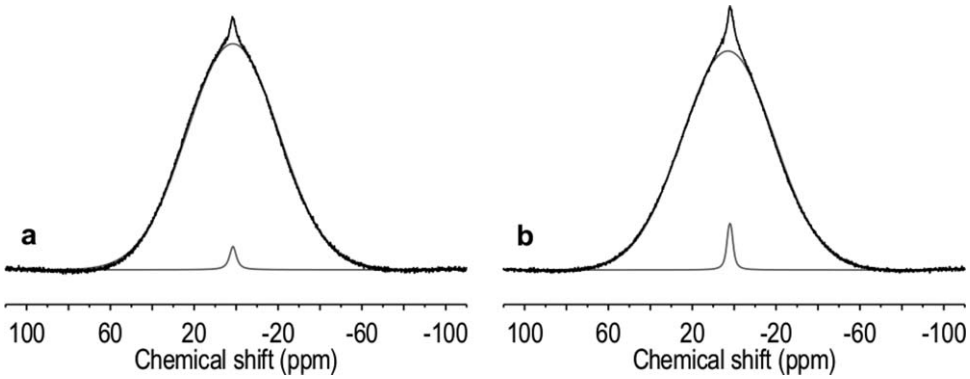

Figure 5. BL ^{1}H-NMR spectra of (a) PLA-Q and (b) PLA-T sample measured at room temperature and deconvolution of the spectra into broad Gaussian and narrow Lorentzian lines.

groups in different crystallographic positions confirm this assumption since they acquire very close values. A significant difference is seen in the relaxation rate of CO carbons. The reason for higher $T_1(^{13}C)$ values for PLA-T(100) sample is the presence of more perfect crystalline domains, as was deduced from narrower lines observed in MAS ^{13}C-NMR spectra and so the larger restriction of the local chain mobility.

^{1}H-NMR Spectra

The PLA-Q at room temperature is an amorphous material, in which the $T_1(^{13}C)$ measurements revealed the presence of CH and CH_3 carbons with different mobility (Table II). To obtain information on the morphology of PLA-Q and PLA-T samples, the BL ^{1}H-NMR measurements were performed at room temperature and at elevated temperatures up to 100 °C.

^{1}H-NMR spectra of solid polymers are broadened mainly due to the strong homonuclear ^{1}H-^{1}H dipolar interaction. Application of MAS technique averages the influence of dipolar interactions, and the information on the chemical shifts of proton species in the sample can be obtained. However, in this way some information on the morphology of the sample is lost. BL ^{1}H-NMR spectra measured bellow glass transition temperature yield a broad line and above glass transition temperature the spectra usually display superposition of a broad and narrow lines which are assigned to a rigid phase of the polymer structure and to regions consisting of highly mobile chains, respectively. If the measurement is performed sufficiently far above glass transition temperature, the line intensities can provide information on the crystallinity of the partially crystalline sample.

At room temperature, which is below PLA glass transition temperature, the BL ^{1}H-NMR spectra of both samples show a broad Gaussian line and a narrow Lorentzian line of a very low intensity (Figure 5). The strongly broadened Gaussian lines with the

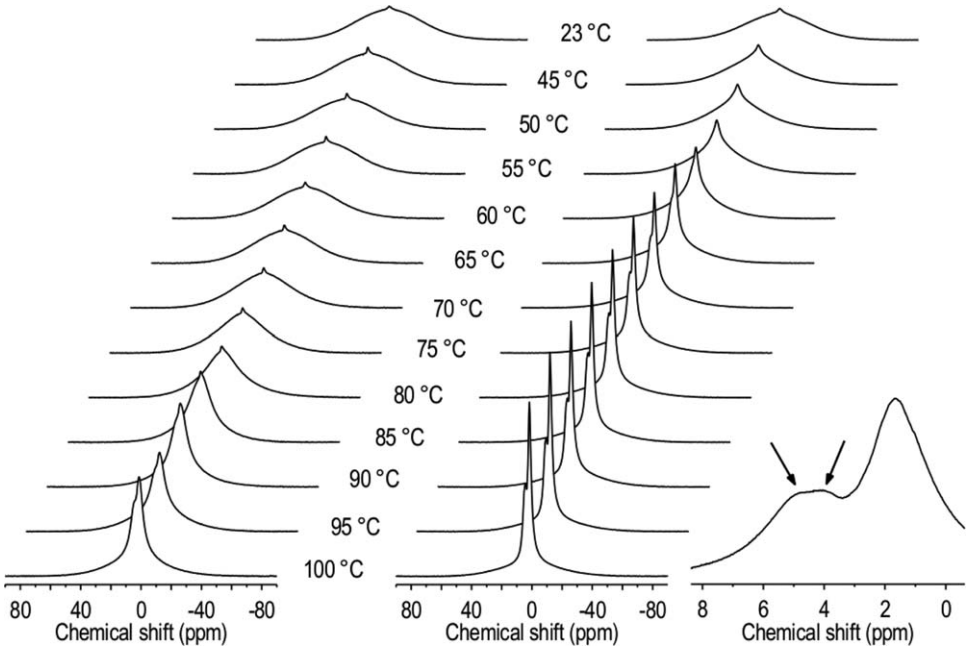

Figure 6. BL ^{1}H-NMR spectra of PLA-Q sample (left) and PLA-T sample (right) measured in the temperature range from room temperature to 100 °C and an enlarged spectrum for PLA-T sample measured at 100 °C (right).

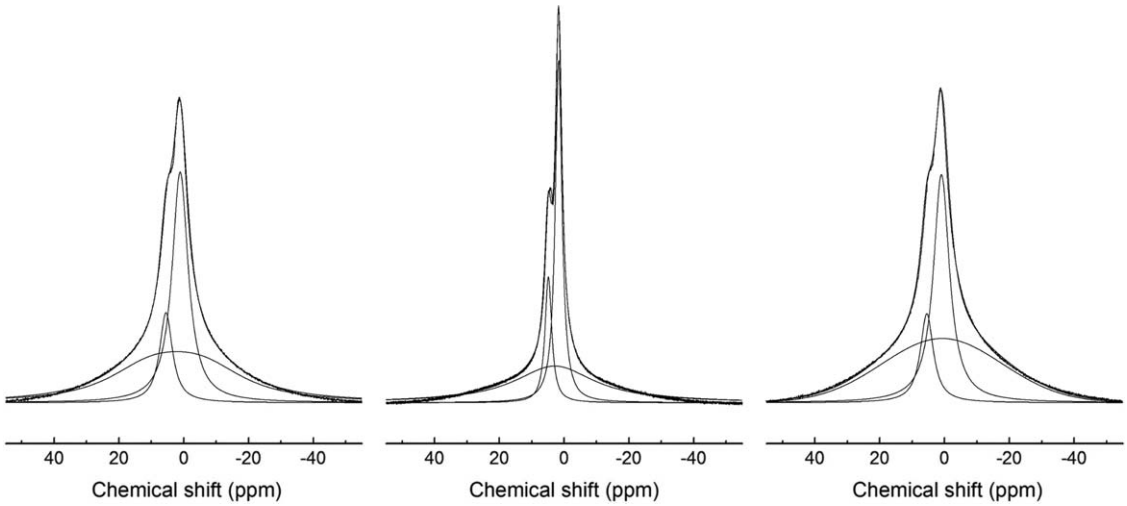

Figure 7. Deconvoluted BL ^{1}H-NMR spectra of PLA-Q (left) and PLA-T (middle) and PLA-V measured at 100 °C.

same widths of 20.7 kHz are at the chemical shifts of approximately 2 ppm. The widths of 1.6 and 1.3 kHz and intensities of 1.0 and 1.7% for PLA-Q and PLA-T were estimated for the Lorentzian lines, respectively indicating the presence of very small fractions within the samples with higher mobility of chains in PLA-T in comparison with PLA-Q even at room temperature.

An increase of temperature within the temperature range above glass transition results in narrowing the spectra (Figure 6) which is related to the glass transition relaxation and the onset of this process is observed at the temperature of 75 °C and 45 °C for PLA-Q and PLA-T, respectively, which can be considered as the glass transition temperatures. The difference in these temperatures indicates that TAC plasticizer facilitates chain motion in PLA. Further heating results in successively increasing amplitudes and areas of narrow lines in the spectra. Moreover, a formation of a shoulder becomes visible in the spectrum at 80 and 60 °C for PLA-Q and PLA-T samples, respectively, and also, in the case of PLA-T, a splitting of the narrow lines into two peaks, which are related to the protons of CH and CH_3 groups,[38] is observed. The difference between the spectra of the studied samples increases approaching 100 °C when the spectrum of the PLA-T sample displays distinctly narrower lines produced by mobile amorphous chains of the polymer. Deconvolution of both spectra at this temperature (Figure 7, Table III) made it possible to determine the fractions of the mobile and rigid chains. However, it has to be taken into account that crystallization could occur within the period of the measurements at elevated temperatures.[15,23,24] Deconvolution of the BL ^{1}H-NMR spectrum of PLA-Q sample required two narrow Lorentzian lines corresponding to CH and CH_3 protons and a broad Gaussian line (Figure 7). Besides lines related to the CH_3 and CH protons of PLA, two overlapping lines in the position of the CH line are observed in the spectrum measured for PLA-T (Figure 6, right). We assume that they come from protons of CH and CH_2 groups within PLA and TAC molecules. The ratio of 2.8:1 of the number of CH_3 protons to the number of CH and CH_2 protons in the PLA-T sample slightly differs from the 3:1 ratio of the number of CH_3 to the number of CH protons in the PLA. Since the CH and CH_2 lines are strongly overlapped, only two narrow Lorentzian lines (one of them related to the CH_3 and the other to the CH and CH_2 protons) were used for deconvolution of the BL ^{1}H-NMR spectrum measured at 100 °C, and in contrast to PLA-Q sample, the rigid fraction of PLA-T gives rise to a broad Lorentzian line (Figure 7, Table III).

The cold crystallization is a gradual process consisting of the formation of a crystalline fraction, so-called α' form[15,24] which cannot be identified using ^{13}C-NMR measurements since its spectrum has the same shape as that of amorphous PLA.[27,37] The disordered crystalline α' form is transformed into the regular α form at elevated temperatures.[12,24] To verify whether the cold crystallization process occured during BL ^{1}H-NMR measurements, the SP ^{13}C-NMR spectra (Figure 8) were measured on the samples at room temperature after BL ^{1}H-NMR

Table III. Widths and intensities (*I*) of Lines Related to the Protons of CH_3 and CH Groups of Mobile Fractions and to Protons of Rigid Fractions in the BL ^{1}H-NMR spectra of PLA-Q, PLA-T, and PLA-V samples measured at 100 °C

	PLA-Q		PLA-T		PLA-V	
Group	Linewidth (kHz)	*I*	Linewidth (kHz)	*I*	Linewidth (kHz)	*I*
CH_3	2.39	0.379	1.00	0.376	2.39	0.368
CH	1.91	0.118	0.99	0.137	1.93	0.116
rigid	16.53	0.503	12.11	0.487	17.52	0.515

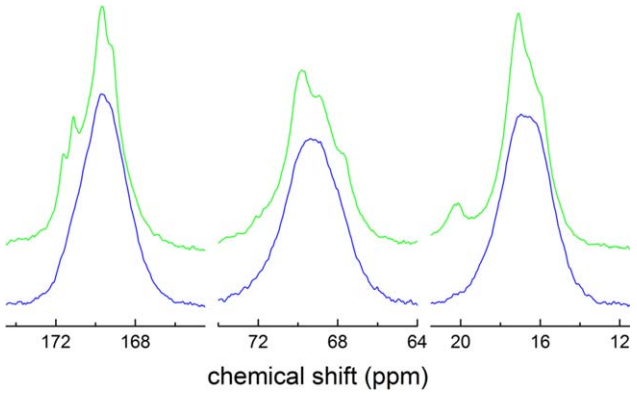

Figure 8. SP ^{13}C-NMR spectra measured at room temperatures for the PLA-Q (bottom) and PLA-T (top) samples after BL ^{1}H-NMR measurements within the temperature range from room temperature up to 100 °C were carried out. [Color figure can be viewed in the online issue, which is available at wileyonlinelibrary.com.]

measurements. The SP ^{13}C-NMR spectrum for the PLA-Q sample does not contain narrow peaks characteristic for the regular crystalline α form of PLA. In contrast, the SP ^{13}C-NMR spectrum of PLA-T shows narrow peaks or shoulders overlapping broad Gaussian lines which prove the formation of the crystalline α form in this sample during ^{1}H-NMR measurements.

For this reason, the broad Gaussian line in the ^{1}H-NMR spectrum of PLA-Q (Figure 7) can be assigned to rigid amorphous fraction and/or crystalline α′ form. The width of the Gaussian line observed at room temperature decreased from 20.7 to 16.5 kHz at 100 °C which indicates mobility enhancement in the rigid fraction. The intensity of this line decreased to 0.50 at 100 °C. The broad Lorentzian line in the ^{1}H-NMR spectrum of PLA-T can be assigned to the rigid amorphous fraction and crystalline α form.

The transformation of the Gaussian line-shape for PLA-Q into Lorentzian for PLA-T can be attributed to the plasticization and/or crystallization process. To determine which of the mentioned processes is responsible for the change in the line shape, deconvolution of the BL ^{1}H-NMR spectrum measured at 100 °C for the virgin semi-crystalline PLA-V sample was carried out. The deconvolution of this spectrum (Figure 7, Table III) provides very similar results to those obtained for the amorphous PLA-Q sample. The Lorentzian lines for the protons in the CH and CH_3 groups show the same widths and the lines assigned to the rigid fraction are of the Gaussian shape for both samples. The percentage of the rigid fraction of PLA-V sample is almost identical with the crystallinity of the sample determined from the ^{13}C-NMR experiments[35] which confirmed the crystalline α form of this sample. The BL ^{1}H-NMR spectra measured for PLA-Q and PLA-V samples also differ in the widths of the Gaussian lines. A broader Gaussian line was observed for the semicrystalline PLA-V sample, when compared with that of the amorphous PLA-Q.

The discussed results indicate that the plasticization of PLA is responsible for the transformation of the Gaussian into Lorentzian line. As mentioned above, the shape of the spectrum at room temperature is Gaussian (the line is characterized by the parameter L/G = 0). The onset of the transformation of the line-shape is at about 65 °C (L/G = 0.2) and at the temperatures above 90 °C the shape of the line related to the rigid fraction with TAC molecules is Lorentzian (L/G = 1). The relative number of TAC protons in the sample is roughly the same as the mass fraction of TAC in PLA-T, and the intensity of 0.487 in Table III can be regarded as the mass fraction associated with a broad Lorentzian line. The influence of plasticization is especially observable through the widths of the particular lines. The data in Table III show that plasticization results in the narrowing of the lines related to the CH and CH_3 protons and to the narrowing of the broad line related to the rigid fraction. It indicates that TAC molecules are present not only in the mobile but also in the rigid fraction and TAC molecules incorporated in the structure of PLA lead to a mobility increase of the chains in both the rigid and the mobile fractions. We assume that TAC molecules incorporated among the chains with restricted mobility facilitate transformation of these chains into the regular crystalline structure. The enhancement of the chain mobility within the part of rigid regions and the simultaneous formation of α crystalline domains lead to the transformation of the line shape from the Gaussian to a relatively broad Lorentzian.

The data in Table III show that the PLA-Q and PLA-V samples comprise the same fractions of very mobile chains. The rigid fraction in PLA-Q heated to 100 °C corresponds to the crystallinity of the semicrystalline PLA-V, its amount is only slightly lower than the crystallinity of the sample prepared by annealing of PLA-Q in the temperature region of cold crystallization.[35] These results indicate that the crystalline α form could arise from the rigid fraction in the process of cold crystallization.

The chain aggregations in the amorphous polymer of lower mobility form the rigid amorphous fraction and could be considered as the starting points of the cold crystallization. The broadening of ^{13}C-NMR lines caused by small dimensions of these aggregations make them undetectable by SP MAS ^{13}C-NMR. Due to the same shape of the ^{1}H-NMR lines for rigid

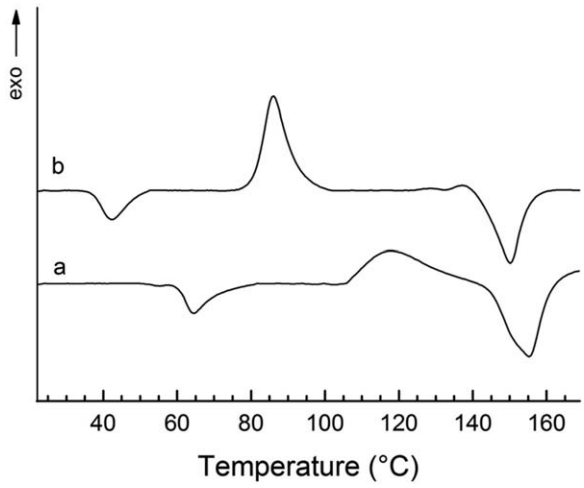

Figure 9. First heating DSC thermograms of PLA-Q (a) and PLA-T (b) samples scanned at the heating rate of 5 °C/min.

Table IV. Glass Transition Temperatures T_g, cold crystallization temperatures T_{cc}, and melting temperatures T_m derived from the first heating DSC scans for PLA-Q and PLA-T samples (Figure 9) as the related peak maximum positions

Sample	T_g (°C)	T_{cc} (°C)	T_m (°C)
PLA-Q	64.4	118.7	155.3
PLA-T	42.5	86.1	150.1

amorphous, α and α′ forms (rigid fraction), these forms are impossible to be distinguished using BL ^{1}H-NMR spectra. The conclusions inferred from the ^{1}H measurements are supported by the results of DSC measurements performed on both PLA-Q and PLA-T samples (Figure 9).

The effect of plasticizer becomes evident in a marked shift of the glass transition and cold crystallization processes to lower temperatures (Table IV) and in obviously faster cold crystallization in PLA-T sample in accordance with[18,21] and with the ^{1}H-NMR measurements discussed above. The glass transition temperatures are observed at 64.4 and 42.5 °C (peak maximum position) for PLA-Q and PLA-T samples, respectively. The cold crystallization process starts above 80 °C for PLA-T and it is finished at 100 °C in contrast to the PLA-Q sample for which the cold crystallization starts only above 100 °C and it overlaps with recrystallization process at temperatures above 120 °C. However, it has to be taken into account that thermal treatment of PLA samples in DSC experiment in which the sample is heated at the rate of 5 °C/min differ from the annealing of samples studied using ^{13}C-NMR and ^{1}H-NMR measurements.

CONCLUSIONS

The SP MAS ^{13}C-NMR measurements performed on quenched and TAC-plasticized PLA samples at room temperature confirmed the amorphous nature of these samples. The annealing of both samples at 80 °C for 48 hours resulted in the formation of crystalline domains; this process was more efficient in TAC-plasticized samples. The annealing at 100 °C resulted in similar crystallinities; however, peaks with narrower linewidths in the spectrum of TAC-plasticized PLA sample were observed. These facts indicate that more perfect crystalline domains were formed in this sample. The TAC plasticizer obviously promotes cold crystallization in PLA structure.

The values of $T_1(^{13}C)$ spin-lattice relaxation times for all studied samples indicate that the presence of TAC molecules leads to an increase of local mobility of PLA chains even at room temperature. During annealing at 100 °C, TAC molecules facilitate formation of more perfect crystalline domains as was inferred from longer $T_1(^{13}C)$ spin-lattice relaxation times for CO carbons in annealed plasticized sample, in comparison with the annealed quenched sample.

The series of BL ^{1}H-NMR spectra performed on quenched and plasticized samples at temperatures up to 100 °C provide very illustrative information on the changes in morphology of the studied samples induced by increasing temperature. The presence of TAC molecules obviously lead to a decrease of the glass transition temperature in a plasticized sample and to an acceleration of formation of crystalline domains. Deconvolutions of the BL ^{1}H-NMR spectra measured at 100 °C make it possible to determine the percentage of the rigid and the mobile phases in both samples. The conclusions drawn from the results obtained using the techniques of NMR spectroscopy are supported by WAXD and DSC measurements.

ACKNOWLEDGMENTS

This research has been supported by the Scientific Grant Agency (VEGA) of the Ministry of Education of the Slovak Republic and the Slovak Academy of Sciences through the project No. 1/0492/13. The authors thank Assoc. Prof. Ján Imrich from Pavol Jozef Šafárik University in Košice, Slovakia, for recording the liquid-state NMR spectrum.

REFERENCES

1. Zhang, J. F.; Sun, X. In Biodegradable Polymers for Industrial Applications; Smith, R., Ed.; CRC Press LLC, Boca Raton, **2005**; Chapter 10, p 251.
2. Avérous, L. In Handbook of Biopolymers and Biodegradable Plastics: Properties, Processing and Applications; Ebnesajjad, S., Ed.; Elsevier, Oxford, **2013**; Chapter 9, p 171.
3. Ren, J., Ed. In Biodegradable Poly(lactic acid): Synthesis, Modification, Processing and Application; Springer: Heidelberg, **2010**; Chapter 6, p 208.
4. Jiang, X.; Luo, Y.; Tian, X.; Huang, D.; Reddy, N.; Yang, Y. In Poly(lactic acid): Synthesis, Structures, Properties, Processing, and Applications; Auras, R. A.; Lim, L.-T.; Selke, S. E. M.; Tsuji, H., Eds.; Wiley, Hoboken, **2011**; Chapter 6, p 69.
5. De Santis, P.; Kovacs, A. *J. Biopolym.* **1968**, *6*, 299.
6. Alemán, C.; Lotz, B.; Puiggali, J. *Macromolecules* **2001**, *34*, 4759.
7. Sasaki, S.; Asakura, T. *Macromolecules* **2003**, *36*, 8385.
8. Wasanasuk, K.; Tashiro, K.; Hanesaka, M.; Ohhara, T.; Kurihara, K.; Kuroki, R.; Tamada, T.; Ozeki, T.; Kanamoto, T. *Macromolecules* **2011**, *44*, 6441.
9. Hoogsteen, W.; Postema, A. R.; Pennings, A. J.; Brinke, G.; Zugenmaie, P. *Macromolecules* **1990**, *23*, 634.
10. Puigali, J.; Ikada, Y.; Tsuji, H.; Cartier, L.; Okihara, T.; Lotz, B. *Polymer* **2000**, *41*, 8921.
11. Cartier, L.; Okihara, T.; Ikada, Y.; Tsuji, H.; Puigali, J.; Lotz, B. *Polymer* **2000**, *41*, 8909.
12. Wasanasuk, K.; Tashiro, K. *Polymer* **2011**, *52*, 6097.
13. Tsuji, H.; Ikada, Y. *Polymer* **1995**, *36*, 2709.
14. Pluta, M.; Galeski, A. *J. Appl. Polym. Sci.* **2002**, *86*, 1386.
15. Tábi, T.; Sajó, I. E.; Szabó, F.; Luyt, A. S.; Kovács, J. G. *eXPRESS Polym. Lett.* **2010**, *4*, 659.
16. Henton, D. E.; Gruber, P.; Lunt, J.; Randall, J. In Natural Fibers, Biopolymers, and Biocomposites; Mohanty, A. K.; Misra, M.; Drzal, L. T., Eds.; CRC Press Taylor & Francis: Boca Raton, **2005**; Chapter 16, p 527.

17. Mekonnen, T.; Mussone, P.; Khalil, H. *J. Mater. Chem.* **2013**, *A, 1*, 13379.
18. Tanrattanakul, V.; Bunkaew, P. *eXPRESS Polym. Lett.* **2014**, *8*, 387.
19. Ljungberg, N.; Wesslén, B. *J. Appl. Polym. Sci.* **2002**, *86*, 1227.
20. Ren, Z.; Dong, L.; Yang, Y. *J. Appl. Polym. Sci.* **2006**, *101*, 1583.
21. Yeh, J. T.; Huang, C. Y.; Chai, W. L.; Chen, K. N. *J. Appl. Polym. Sci.* **2009**, *112*, 2757.
22. Pan, P.; Yang, J.; Shan, G.; Bao, Y.; Weng, Z.; Cao, A.; Yazawa, K.; Inoue, Y. *Macromolecules* **2012**, *45*, 189.
23. Henricks, J.; Boyum, M.; Zheng, W. *J. Therm. Anal. Calorim.* **2015**, *120*, 1765.
24. Li, Q.; Zhang, R.; Shao, C.; Wang, Y.; Shen, C. *Polym. Eng. Sci.* **2015**, *55*, 359.
25. Thakur, K. A. M.; Kean, R. T.; Zupfer, J. M.; Buehler, N. U. *Macromolecules* **1996**, *29*, 8844.
26. Ito, T.; Maruhashi, Y.; Demura, M.; Asakura, T. *Polymer* **2000**, *41*, 859.
27. Pan, P.; Zhu, B.; Dong, T.; Yazawa, K.; Shimizu, T.; Tansho, M.; Inoue, Y. *J. Chem. Phys.* **2008**, *129*, 184902.
28. Tsuji, H.; Kamo, S.; Horii, F. *Polymer* **2010**, *51*, 2215.
29. Nishida, M.; Nishimura, Y.; Tanaka, T.; Oonishi, M. *J. Appl. Polym. Sci.* **2012**, *123*, 1865.
30. Pawlak, T.; Jaworska, M.; Potrzebowski, M. *J. Phys. Chem. Chem. Phys.* **2013**, *15*, 3137.
31. Chen, Q.; Hou, S. S.; Schmidt-Rohr, K. *Solid State Nucl. Magn. Reson.* **2004**, *26*, 11.
32. Broz, M. E.; VanderHart, D. L.; Washburn, N. R. *Biomaterials* **2003**, *24*, 4181.
33. Nozirov, F.; Nazirov, A.; Jurga, S.; Fu, R. *Solid State Nucl. Magn. Reson.* **2006**, *29*, 258.
34. Ando, S.; Harris, R. K.; Holstein, P.; Reinsberg, S. A.; Yamauchi, K. *Polymer* **2001**, *42*, 8137.
35. Olčák, D.; Hronský, V.; Kovaľaková, M.; Vrábel, P.; Chodák, I.; Alexy, P. *Int. J. Polym. Anal. Ch.* **2015**, *20*, 396.
36. Fung, B. M.; Khitrin, A. K.; Ermolaev, K. *J. Magn. Reson.* **2000**, *142*, 97.
37. Torchia, D. A. *J. Magn. Reson.* **1978**, *30*, 613.
38. Carrasco, F.; Pagès, P.; Gámez-Pérez, J.; Santana, O. O.; Maspoch, M. L. *Polym. Degrad. Stabil.* **2010**, *95*, 2508.